Resonant photoemission in Ti_2O_3 and V_2O_3: Hybridization and localization of cation 3*d* orbitals

Kevin E. Smith* and Victor E. Henrich
Applied Physics, Yale University, 15 Prospect Street, New Haven, Connecticut 06520
(Received 2 June 1988)

Resonant photoemission from cation 3*d* and oxygen 2*p* states in both Ti_2O_3 and V_2O_3 single crystals has been observed as the photon energy is swept through the cation $3p \rightarrow 3d$ optical-absorption transition. These nonmaximal valency oxides are excellent materials in which to study the effect of a ligand environment on resonant photoemission from cation *d* states, due to the existence of partially occupied *d* states well separated from the O 2*p* states. This investigation has revealed complex new aspects of the electronic structure of these oxides and the phenomenon of resonant photoemission in them. The cation 3*d* resonant emission was found to display a strong angular anisotropy which could be related to the molecular-orbital structure of these oxides. The maximum in the cation 3*d* resonance emission occurs at the same photon energy in both the metals and oxides, indicating a significant degree of localization of the cation resonance. A strong resonance in the O 2*p* emission from Ti_2O_3 is observed as the photon energy is swept through the Ti $3p \rightarrow 3d$ transition. A much smaller resonance is seen in the O 2*p* emission from V_2O_3 at the V $3p \rightarrow 3d$ transition, despite an increase in *d* character in the O 2*p* band in V_2O_3. Thus caution must be used in extracting information on hybridization from resonant photoemission data.

I. INTRODUCTION

The phenomenon of resonant photoemission in transition metals and their compounds has been the subject of numerous investigations of late.[1] This interest has a variety of origins. Studies of the phenomenon itself are significant since the details of the resonance in a number of metals and compounds are not fully understood. Additionally, resonant photoemission is being used increasingly as a method of isolating the *d*-state contribution to complex hybridized ligand states.

Recently, it was discovered that the $3p \rightarrow 3d$ resonance in the light transition metals Ti, V, and Cr is very different from that in the heavier transition metals.[2–4] These resonances were found to extend over 40–50 eV in photon energy as opposed to approximately 10 eV in the heavier metals. Also, the resonance profiles (plots of emission intensity versus photon energy) in the lighter metals do not display the characteristic Fano-type line shapes seen for the heavier metals. Finally, the resonance displays a delay in onset to photon energies larger than the $3p \rightarrow 3d$ energy-level separation, which does not occur in the heavier metals. Consequently, it was decided to examine the resonance in well-characterized oxides of Ti and V in order to examine the effect of a ligand field on these unusual properties of the resonance in these atoms. It was also hoped to use the resonance to identify the extent of *d*-state hybridization in the O 2*p* bands in oxides of these metals.

We report here the results of a study of resonant photoemission from single crystal Ti_2O_3 and V_2O_3 (both pure and Cr doped).[5] The cation $3p \rightarrow 3d$ resonance was measured in both angle-integrated and angle-resolved modes. Significant differences are observed between the profiles measured with the angle-resolved detector oriented parallel to the axis of an occupied molecular orbital in Ti_2O_3 and those measured with the detector oriented away from this axis. The resonance onset in both materials displays a delay to photon energies greater than the $3p \rightarrow 3d$ energy-level separation that is smaller than in the corresponding metal; however, the photon energy at which the resonance maximizes in an angle-integrated mode is identical for both oxides and metals. Finally, a large resonance in the emission from the O 2*p* states in Ti_2O_3 was observed that is inconsistent with the known hybridization properties of these materials.

In Sec. II we present a brief review of the electronic structure of Ti_2O_3, V_2O_3, and Cr-doped V_2O_3. In Sec. III we discuss the origins or resonant photoemission. Section IV contains a brief description of the experimental apparatus used. The results of the experiment and a discussion of the data obtained are presented in Secs. V and VI, respectively. The paper concludes with a summary in Sec. VII.

II. ELECTRONIC STRUCTURE OF Ti_2O_3, V_2O_3, AND Cr-V_2O_3

The electronic structure of Ti_2O_3 and V_2O_3 has recently been the subject of a detailed investigation using angle-integrated and angle-resolved photoemission, and synchrotron radiation.[6] The electronic structure and properties of Cr-doped V_2O_3 have been reviewed by Kuwamoto *et al.*[7] Here we will briefly restate some of the more important points concerning the electronic properties of these materials; the reader is referred to Refs. 6 and 7 for more comprehensive discussions of these topics.

Room-temperature Ti_2O_3 and V_2O_3 both have the corundum structure with a trigonal (rhombohedral) Bra-

 ©1988 The American Physical Society

vais lattice; the unit cell contains a 10-atom basis set.[8] When doped with Cr, V_2O_3 retains the corundum structure at room temperature, with the Cr entering the lattice substitutionally.[7] Single crystals of these oxides have only one cleavage plane: $(10\bar{1}2)$ using hexagonal notation.[9,10] The trigonal crystal field splits the atomic $3d$ states into a pair of e_g^σ orbitals, a pair of e_g^π orbitals, and an a_{1g} orbital. The a_{1g} orbital is directed along the hexagonal c axis, forming a covalent molecular bond between pairs of metal ions. The e_g^π orbitals are involved in bonding between metal atoms in the basal plane and the e_g^σ orbitals are directed towards nearest-neighbor oxygen atoms.[8]

At room temperature Ti_2O_3 is a semiconductor with a 0.1-eV band gap separating the full a_{1g} band from the empty e_g^π band; the Ti^{3+} cations are in a $3d^1$ configuration, with one d electron per cation (see Fig. 1 of Ref. 6). In contrast, V_2O_3 is metallic at room temperature with both the a_{1g} and the e_g^π bands partially occupied; the V^{3+} cations are in a $3d^2$ configuration, with two d electrons per cation. The electronic state of V_2O_3 doped with Cr is critically dependent on the Cr concentration and the temperature. These materials all undergo a number of metal-insulator transitions; in Cr-doped V_2O_3 these transitions can change the symmetry of the lattice.[8] We have studied two Cr-doped V_2O_3 samples with dopings of 1.5 and 3 at. % Cr. At room temperature both of these samples are insulators, whereas pure V_2O_3 is metallic.[7]

III. RESONANT PHOTOEMISSION

A. General considerations

Resonant photoemission from atomic $3d$ states occurs when the energy of the ionizing photons coincides with the $3p \rightarrow 3d$ optical-absorption threshold. As the photon energy is changed from below to above this threshold, the $3d$ photoelectron yield is observed to increase dramatically. This phenomenon has been extensively investigated in both atoms and solids, and a comprehensive review has been published recently by Davis.[1] In large part, these studies have concentrated on the phenomenon in the rare-earth metals and heavy ($Z > 25$, Z denoting atomic number) transition metals. Far fewer studies of the resonance in the light transition metals Ti, V, and Cr have been undertaken.

The enhancement of the $3d$-photoelectron yield at photon energies close to the $3p \rightarrow 3d$ absorption threshold is due to the existence, at these energies, of a separate ionization mechanism which leaves the system in the same final state as does conventional photoemission. For emission from a d state, the latter process can be written in an atomic picture, as

$$3p^6 3d^n + h\nu \rightarrow 3p^6 3d^{n-1} + e^-(\varepsilon) ,$$

where a photon of energy $h\nu$ ionizes the neutral atom and ejects a $3d$ electron with kinetic energy ε. $3p$ optical absorption can be written as

$$3p^6 3d^n + h\nu \rightarrow [3p^5 3d^{n+1}]^* ,$$

where the photon energy $h\nu$ is close to the $3p$ threshold and where the asterisk denotes an excited state. The $[3p^5 3d^{n+1}]^*$ state consists of a hole in the $3p$ shell of a metal atom and an extra electron in the d shell of the same atom. This excited state can deexcite by a number of mechanisms. Following the notation of Bertel *et al.*,[3] one such mechanism is autoionization,

$$[3p^5 3d^{n+1}]^* \rightarrow [3p^5 3d^n]^* + e^-(\varepsilon') ,$$

followed by a super-Coster-Kronig (SCK) Auger decay,

$$[3p^5 3d^n]^* \rightarrow 3p^6 3d^{n-2} + e^-(\varepsilon'') ,$$

where ε'' is the kinetic energy of the d electron emitted in the $M_{2,3}M_{4,5}M_{4,5}$ Auger event. Since the energies of the emitted electrons in this decay channel are different from the energy of the photoemitted electron, no resonance occurs.

In competition with this mechanism is direct recombination,

$$[3p^5 3d^{n+1}]^* \rightarrow 3p^6 3d^{n-1} + e^-(\varepsilon) .$$

Here the final state and the electron kinetic energy are identical to those following conventional $3d$ photoemission. This direct recombination interferes with the conventional $3d$ photoemission process and produces a characteristic narrow, asymmetrical line shape, called a Fano line shape,[11] for the resonance profile (emission intensity versus photon energy). The location of the maximum of the resonance profile in energy differs somewhat from the energy of the transition involved in the resonance.[11]

Electrons are emitted by direct recombination from d states independent of the mechanism producing the $3p$ hole. Thus, direct-recombination features are observed in both Auger and electron-energy-loss spectra once a $3p$ hole exists.[1]

B. Light transition metals—Ti,V,Cr

The resonant-photoemission process becomes more complicated when one moves from an isolated atomic or ionic system to a solid. Barth *et al.*[2] have dramatically illustrated this point by comparing the $3p \rightarrow 3d$ resonance profiles from Cr^+ vapor[12] and Cr metal.[13] In the vapor, the resonance has a classic Fano line shape with a width of 2–3 eV, while in the metal the profile is 40–50 eV wide, with no clearly defined Fano line shape. This large width in photon energy indicates that the $3p \rightarrow 3d$ resonance occurs over a range of photon energies much greater than would be expected from a resonance due to a simple interference. Barth *et al.*[2] explain this using a model of shakeup excitations accompanying the $3p \rightarrow 3d$ optical absorption. These shakeup excitations essentially act as losses, thereby requiring a higher photon energy to achieve resonance than in their absence. However, as one moves across the $3d$-transition-metal series, the profiles become more Fano-like; the resonance profile in Ni is quite well described by a Fano line shape.[14]

Another important difference between the resonance in light transition metals and the heavier metals is the larger delay in the onset of the resonance to photon energies

above the $3p \rightarrow 3d$ energy-level separation that occurs in the light transition metals.[1-4] In a simple one-electron picture, resonance would be expected to occur when the photon energy equals the difference in binding energies of the filled $3p$ level and the empty $3d$ state. This implies that the resonance should occur at photon energies close to 33 eV for Ti and 37 eV for V; in fact, the resonance profiles peak at 47 eV for Ti and 50 eV for V.[2]

Delays in the onset of resonance have been observed previously in the $4d \rightarrow 4f$ transition in the rare-earth elements.[15] These delays have been explained by Dehmer *et al.*[16] in terms of the exchange interaction between the $4d$ hole and $n+2$ $4f$ electrons. The $4d$ and $4f$ wave functions overlap significantly in the lighter rare-earth metals where the $4f$ wave function is collapsed. The exchange interaction then splits the multiplet structure of the atom and raises some multiplets by as much as 20 eV.[16] Bertel *et al.*[3,4] have postulated that a similar effect occurs in the light $3d$ transition metals. Here, a collapsed $3d$ wave function overlaps a $3p$ wave function. Again, the exchange interaction (this time between a $3p$ hole and $n+1$ $3d$ electrons) causes the resonance to peak far above threshold by raising the optically favored $3p^5 3d^{n+1}$ multiplets. However, Bringans and Hochst[17] have pointed out that the variation in the $3p,3d$ exchange interaction alone is not sufficient to explain the observed variation in the magnitude of the delay in onset as one moves across the $3d$ transition metals from Ti to Cu.[2]

The shape of the resonance profiles from Ti and V differ significantly.[2] For Ti the profile consists of a sharp rise at the onset of the resonance, maximizing at approximately 47–48 eV photon energy, followed by a broad plateau and a second maximum at approximately 59 eV.[2] The plateau and second maximum are due to multielectron excitations (losses) in the model of Barth *et al.*[2] The intensities of the resonance peak (i.e., the peak closest to onset for which no losses need be invoked to explain its energy location) and the loss peak (i.e., the peak for above onset which is explicable only by considering shakeup) are roughly equivalent in the profile from Ti.[2] For V the resonance peak occurs at approximately 50 eV, with the loss peak appearing at around 65 eV.[2] Thus, in going from Ti to V the separation of these features increases significantly. Additionally, in V the relative intensities of the resonance and loss peaks change dramatically from that seen in Ti; the loss peak dominates the profile, with the peak just above resonance appearing as little more than a shoulder.[2]

As was mentioned earlier, the location in photon energy of the maximum nearest to the onset in a resonance profile is not exactly the binding energy of the $[3p^5 3d^{n+1}]^*$ state. (The difference between the true resonance energy and the peak in the profile is a function of q, an asymmetry parameter in Fano's theory.[11]) The difference is expected to be small, but without a well-defined Fano line shape in the experimentally derived profiles, quantifying this difference is difficult. The resonance energies (i.e., binding energies of the $[3p^5 3d^{n+1}]^*$ excited states) measured from the resonant-photoemission profiles agree well with the results of other measurements; in electron-energy-loss spectroscopy (EELS), losses are observed at approximately 47–48 eV for Ti (Refs. 4 and 18–20) and 48–53 eV for V (Refs. 20–22). These losses are related to the $3p \rightarrow 3d$ transition and their energies correspond well with the peaks in the resonance profiles. Similarly, there is agreement between the energy location of the $3p$ optical-absorption peaks for Ti and V (Refs. 22 and 23) and the resonance-profile peaks.

C. Ti and V compounds

Resonant photoemission has been studied in a small number of Ti and V compounds. The Ti compounds that have been studied are oxidized Ti metal,[3,4] polycrystalline TiN_2,[17] and single-crystal TiS_2 and its intercalate compounds $Fe_{1/3}TiS_2$ and $Ni_{1/3}TiS_2$.[24] Additionally, resonant photoemission has been observed previously from single-crystal Ti_2O_3 (Refs. 6 and 18) and from single-crystal $SrTiO_3$ (Ref. 25). Prior to this work, the only vanadium compound from which resonant photoemission has been observed was single-crystal VN.[26] The resonance process in these materials will be discussed in Sec. VI when the results of our investigation of Ti_2O_3 and V_2O_3 are analyzed. At this stage it is sufficient to note that there are no significant changes observed in the $3p \rightarrow 3d$ resonance in going from the pure metals to the compounds studied previously.

IV. EXPERIMENTAL METHODS

A. Apparatus

All the experiments reported here were performed on beamline U14 at the National Synchrotron Light Source, Brookhaven National Laboratory. Details of the experimental apparatus have been published previously.[6] Angle-integrated photoemission spectra were obtained using a Physical Electronics double-pass cylindrical-mirror analyzer (CMA), and angle-resolved spectra were taken using a Vacuum Generators (VG) hemispherical electron spectrometer. Both spectrometers are mounted in the same ultrahigh-vacuum (UHV) chamber (base pressure $< 1.5 \times 10^{-10}$ Torr). A flux monitor, consisting of a high-transmission gold-coated metal grid in front of a channeltron electron multiplier, was used to measure the incident-photon-beam intensity. Unless otherwise indicated, all data presented here are normalized to the photon flux. No attempt was made to account for the transmission functions of the analyzers. All energy-distribution curves (EDC's) are referenced to the Fermi level, E_F, which was determined from an atomically clean gold foil. All angle-resolved spectra were taken with the photon beam incident at 45° to the sample normal, giving roughly equal s and p polarization for the photon beam; angle-integrated spectra were taken with the beam incident at about 60° to the sample normal. Resonance profiles were measured by taking a series of EDC's at different photon energies and integrating the area above background under a given emission feature.

B. Sample preparation

The single-crystal Ti_2O_3 used in this experiment was grown by T.B. Reed of Lincoln Laboratory. The V_2O_3 was grown by D. Buttrey of Purdue University. The Cr-doped V_3O_3 single crystals were provided by J.M. Honig, also of Purdue University. Each material cleaves to expose the $(10\bar{1}2)$ surface.[9,10] In general, Ti_2O_3 cleaves much better than either pure or Cr-doped V_2O_3. Good (1×1) low-energy electron-diffraction (LEED) patterns are obtained from each material following cleavage, with those from Ti_2O_3 being of higher quality than those from the vanadium oxides. All crystals were cleaved in the experimental chamber at pressures $<1.5\times10^{-10}$ Torr. Further details of the sample preparation can be found in Ref. 6.

V. RESULTS

Angle-integrated photoemission spectra for $Ti_2O_3(10\bar{1}2)$ taken with photon energies between 34 and 70 eV are shown in Fig. 1. The emission just below E_F is from the Ti $3d$ states (a_{1g} band); the width of this feature is approximately 1.5 eV. The large emission feature between 4 and 10 eV below E_F is derived predominantly from the O $2p$ states. Angle-integrated and angle-resolved normal-emission spectra from $Ti_2O_3(10\bar{1}2)$ surfaces taken from various photon energies have been published previously;[6,18] however, in both cases no flux monitor was used and the spectra were normalized to the area under the O $2p$ emission. As will be shown below, the assumption that the O $2p$ emission intensity does not vary appreciably with photon energy is incorrect. [In the case of the normal-emission spectra published previously,[6] the emphasis was on band dispersion (i.e., binding energy) rather than the absolute intensities of emission features, so the conclusions of that publication remain unchanged.] The angle-resolved normal-emission spectra from $Ti_2O_3(10\bar{1}2)$ taken during the present experiments are similar to the earlier ones,[6] and so are not presented here. In addition, angle-resolved spectra were taken with the detector oriented 55° off the sample normal, along the (0001) axis of the crystal, for various photon energies; the motivation for this will be discussed in the next section. (The crystal orientation was determined by Laue x-ray diffraction prior to introduction of the sample into the UHV chamber.) These spectra are quite similar to the normal-emission spectra of Ref. 6, so they are not presented here.

Angle-integrated photoemission spectra for $V_2O_3(10\bar{1}2)$ taken with photon energies between 36 and 80 eV are shown in Fig. 2. This crystal of V_2O_3 is nominally doped with 3 at.% Cr. Angle-integrated and angle-resolved spectra of pure V_2O_3 (normalized to a constant O $2p$ emission intensity) have been published previously.[6] Few differences in the photoemission spectra taken at room temperature from pure V_2O_3 and V_2O_3 doped with 1.5 and 3 at.% Cr could be detected beyond a rigid shift of the spectra away from E_F in the Cr-doped samples.[27] Emission from the V $3d$ states is visible close to E_F; this feature is about 3.5 eV wide. Below the V $3d$ band, between 4 and 10 eV below E_F, lies emission from the predominantly O $2p$ states. No clear gap can be observed in the spectra between the V $3d$ and O $2p$ emission; this absence of a gap where one is theoretically predicted has been discussed in Ref. 6. Angle-resolved normal-emission spectra were also recorded from V_2O_3 while the photon flux was monitored; these are similar to the spectra of Ref. 6, and are consequently not shown. The resonant behavior of the V $3d$ and O $2p$ emission from both pure and Cr-doped V_2O_3 is very similar, and for the remainder of this paper we will not distinguish between the samples and refer to them all as V_2O_3.

Figure 3 shows the photon-energy dependence of the Ti $3d$ emission (integrated area above background) from Ti_2O_3 as measured in an angle-integrated mode and the two angle-resolved modes discussed above, normal to the

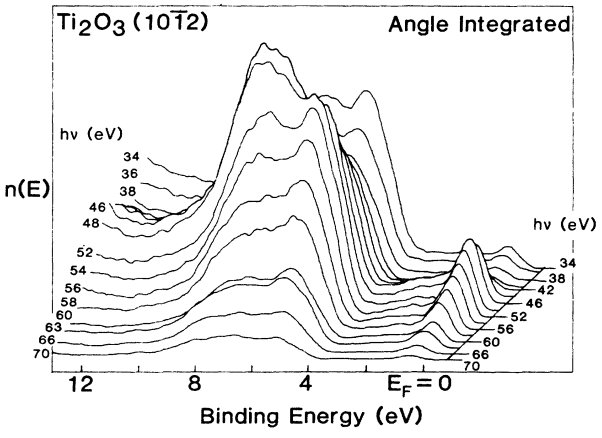

FIG. 1. Series of angle-integrated photoemission spectra from $Ti_2O_3(10\bar{1}2)$ taken for photon energies between 34 and 70 eV.

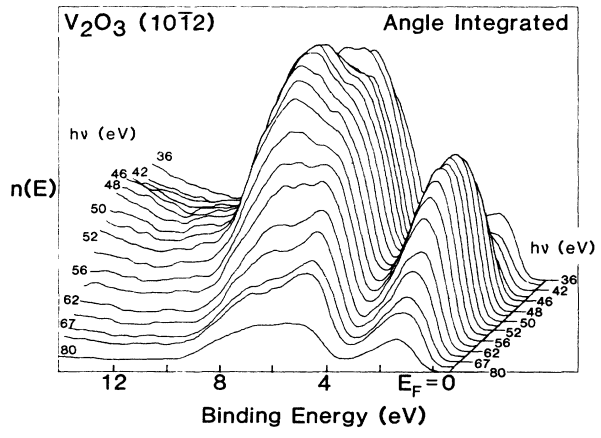

FIG. 2. Series of angle-integrated photoemission spectra from $V_2O_3(10\bar{1}2)$ taken for photon energies between 36 and 80 eV.

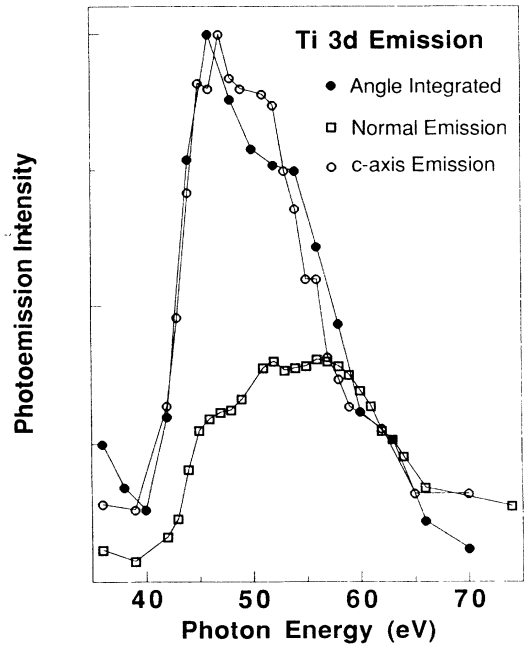

FIG. 3. Photon-energy dependence of the Ti $3d$ emission from $Ti_2O_3(10\bar{1}2)$ as measured in an angle-integrated mode, in an angle-resolved normal-emission mode, and in an angle-resolved mode where the detector is set 55° off normal, along the bulk c-axis direction. See text for details.

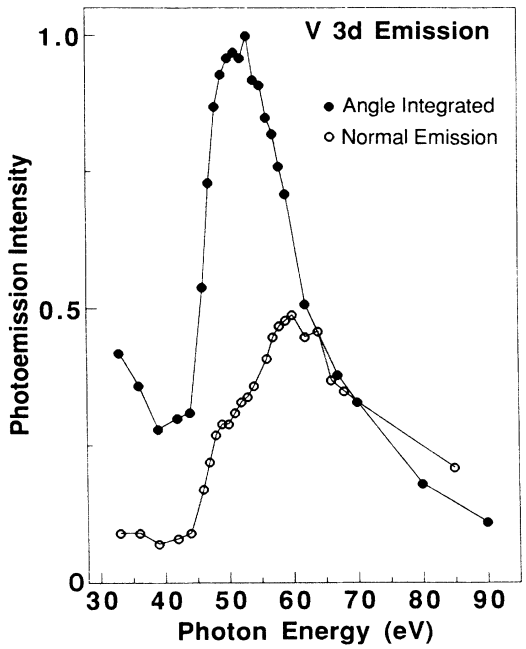

FIG. 4. Photon-energy dependence of the V $3d$ emission from $V_2O_3(10\bar{1}2)$ as measured in angle-integrated and angle-resolved normal-emission modes.

$(10\bar{1}2)$ plane and along the bulk c axis. The angle-integrated profile and that taken for emission along the bulk c axis are set to the same maximum peak height; the profile from the normal-emission experiments is scaled so that the slopes of all three profiles coincide at higher photon energies. Independent of scaling, it is clear that both the angle-integrated profile and the angle-resolved profile taken with the detector along the c axis have a maximum at a photon energy of approximately 47 eV. In contrast, the normal-emission profile shows only a shoulder at this energy and maximizes at a photon energy of 56 eV. In each profile the onset of the resonance occurs for photon energies greater than the $3p \rightarrow 3d$ energy-level separation of 36.5 eV.[27]

The corresponding photon-energy dependence of the V $3d$ emission from V_2O_3 is shown in Fig. 4 for angle-integrated and angle-resolved normal-emission modes of detection. (Angle-resolved spectra with the detector parallel to the bulk c axis were not taken for V_2O_3.) As in Fig. 3, the data have been scaled so that the slopes of the two profiles are similar at higher photon energies. The same general shift of the maximum in the resonance profiles between angle-integrated and normal-emission measurements that was observed for Ti_2O_3 occurs for the V $3d$ emission from V_2O_3. The profile maximizes at approximately 52 eV in the angle-integrated case and at 60 eV in the normal-emission mode. These is a delay in the onset of the resonance to photon energies greater than the $3p \rightarrow 3d$ energy-level separation of 40.5 eV.[27]

Figure 5 presents the photon-energy dependence of the emission from the O $2p$ valence band in Ti_2O_3 as measured in both angle-integrated and angle-resolved normal-emission modes; the corresponding Ti $3d$ data are also shown for comparison. The O $2p$-emission intensity increases by approximately 100% when the photon energy is swept through the Ti $3p \rightarrow 3d$ resonance. This is a remarkable result and will be discussed in Sec. VI. Also noteworthy in Fig. 5 is the similarity in the resonance profiles from the O $2p$ states when measured in either angle-integrated or normal-emission modes. This contrasts with the Ti $3d$ profiles, which show the significant

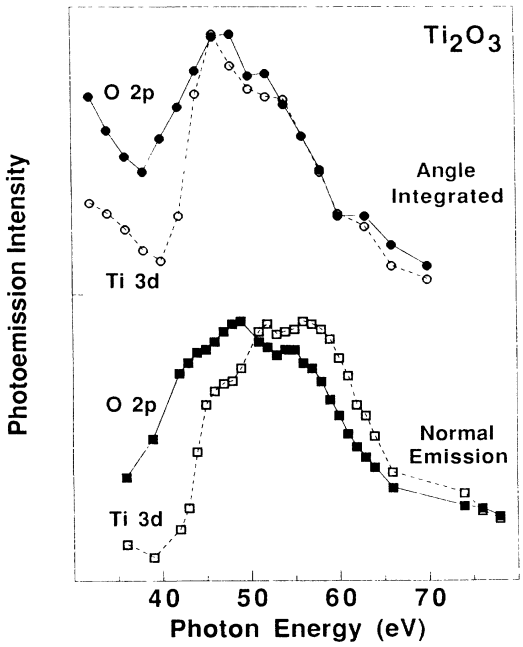

FIG. 5. Photon-energy dependence of the Ti $3d$ and O $2p$ emission from $Ti_2O_3(10\bar{1}2)$ as measured in angle-integrated and angle-resolved normal-emission modes.

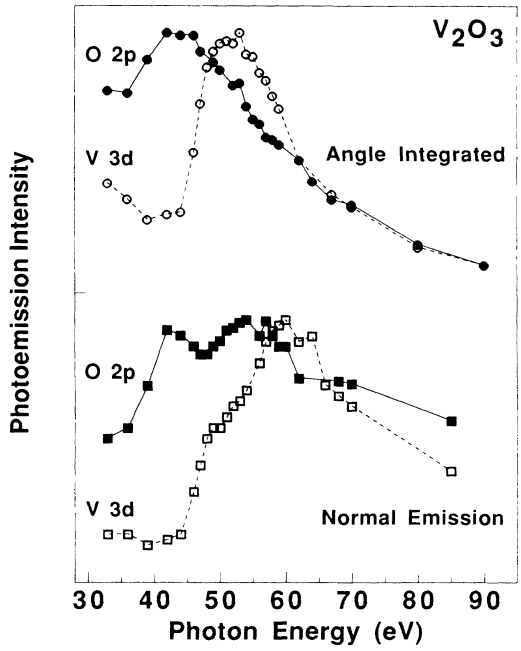

FIG. 6. Photon-energy dependence of the V $3d$ and O $2p$ emission from $V_2O_3(10\bar{1}2)$ as measured in angle-integrated and angle-resolved normal-emission modes.

changes discussed above.

The corresponding photon-energy dependence of the O $2p$ emission from V_2O_3 is presented in Fig. 6. As in Fig. 5, resonance profiles measured in both angle-integrated and normal-emission modes are shown for both O $2p$ and V $3d$ emission. The resonance in the O $2p$ emission in V_2O_3 upon sweeping the photon energy through the V $3p \rightarrow 3d$ transition is much smaller than the corresponding resonance in Ti_2O_3, particularly for the angle-integrated case; the significance of this will be discussed later. Also of importance is the observation that the O $2p$ profiles peak at approximately 10 eV lower photon energies than do the V $3d$ profiles. This is in sharp contrast to the Ti_2O_3 measurement, where the Ti $3d$ and O $2p$ profiles both maximize at almost identical photon energies in the angle-integrated mode.

Partial-yield spectra were also recorded from Ti_2O_3 and V_2O_3. In a partial-yield experiment, only electrons that have been inelastically scattered are detected, and the photon energy is swept through a core-level optical-absorption transition. Partial-yield spectra are known to be very similar to optical-absorption spectra.[28] In these experiments we monitored the intensity of electrons emitted with 5 eV kinetic energy and swept the photon energy through the cation $3p \rightarrow 3d$ optical-absorption region. Figure 7 shows the partial-yield spectra from Ti_2O_3 measured in an angle-resolved mode for both normal emission and for the detector set along the c axis. Figure 8

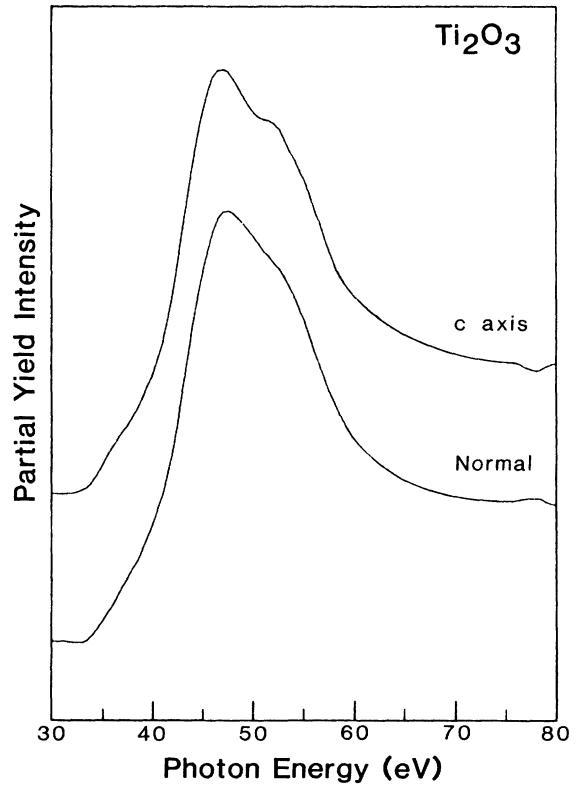

FIG. 7. Partial-yield spectra for $Ti_2O_3(10\bar{1}2)$ measured in normal emission and with the detector set along the direction of the bulk c axis (55° off normal). Kinetic energy is 5 eV.

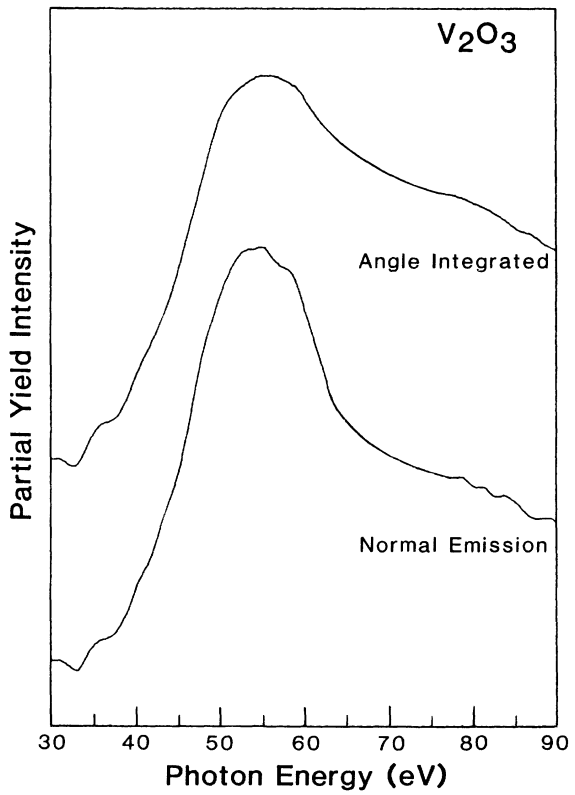

FIG. 8. Partial-yield spectra from $V_2O_3(10\bar{1}2)$ measured in angle-integrated and normal-emission modes. Kinetic energy is 5 eV.

shows the partial-yield spectra from V_2O_3 measured in both angle-integrated and normal-emission modes. Independent of the mode of measurement, the partial-yield spectra show a single peak located at 47 eV in Ti_2O_3 and 55 eV in V_2O_3.

VI. DISCUSSION

The discussion of the data presented in the preceding section can conveniently be divided between analysis of the resonance behavior of the cation $3d$ emission and that of the O $2p$ emission.

A. Cation $3d$ resonance

1. Angular effects

The resonance profiles from both the Ti $3d$ and V $3d$ states, plotted in Figs. 3 and 4 respectively, display significant differences as a function of the mode and angle of measurement. When the cation $3d$ profiles are measured in normal emission from a $(10\bar{1}2)$ surface, the emission maximizes at 8–9 eV higher photon energies than for the corresponding angle-integrated measurement. The partial-yield spectra of Figs. 7 and 8 indicate only a single peak in the optical absorption corresponding to the cation $3p \rightarrow 3d$ transition. The photon energies for which the partial-yield spectra maximize (47 eV for Ti_2O_3, 55 eV for V_2O_3) are very similar to the maxima in the angle-integrated resonance profiles (47 eV for Ti_2O_3, 52 eV for V_2O_3). Additionally, the EELS spectrum of Ti_2O_3 shows a peak at 47.5 eV.[18] Thus, we assign the peak at 47 eV in the angle-integrated Ti $3d$ resonance profile from Ti_2O_3 to the Ti $3p \rightarrow 3d$ transition. Similarly, the peak at 52 eV in the angle-integrated V $3d$ resonance profile from V_2O_3 is assigned to the V $3p \rightarrow 3d$ transition. The implications of the photon energy at which these peaks occur is discussed below; here we will concentrate on the origins of the differences between the angle-integrated and normal-emission profiles. If the cation $3p \rightarrow 3d$ transition occurs at the photon energy determined in the angle-integrated measurements, then why do the maxima in the normal-emission profiles occur at much higher photon energies?

The normal-emission profiles (Figs. 3 and 4) both display shoulders at the location of the $3p \rightarrow 3d$ resonance; the maxima in these profiles lie in the photon-energy range where multielectron excitations have to be invoked in order to explain the resonant behavior.[2] We can consider the shift in energy of the maxima in the normal-emission profile as either an increase in the intensity of the electrons being emitted at the higher photon energies, or a decrease in the number being emitted close to onset (i.e., at the $3p \rightarrow 3d$ transition), where loss processes are not involved. As will be shown below, we have determined that it is primarily the latter phenomenon that occurs and that the structure in the $3d$ resonance profiles close to the onset of the $3p \rightarrow 3d$ resonance displays a larger sensitivity to the molecular-orbital structure of these oxides.

As was discussed in Sec. II, only the a_{1g} orbital is occupied in Ti_2O_3. This molecular orbital is similar to the atomic d_{z^2} orbital, with lobes of charge pointing along the hexagonal c axis. In the corundum lattice, the normal to a $(10\bar{1}2)$ plane makes an angle of $\simeq 55°$ with the c axis. Consequently, the a_{1g} orbitals are directed far away from the detector in a normal-emission experiment from a $(10\bar{1}2)$ surface. Hence, if electrons are preferentially photoemitted along the direction of a molecular orbital, few electrons from the a_{1g} orbital should reach the detector in the normal-emission experiment. For the angle-integrated measurements made with a CMA, the a_{1g}-orbital direction is inside the acceptance cone of the analyzer, and electrons from this orbital should be detected.

To test this idea, the angle-resolved detector was rotated into the direction of the bulk c axis and the Ti $3d$ resonance profile from Ti_2O_3 measured; this profile is shown in Fig. 3. The profile obtained in this mode is almost identical to that obtained in the angle-integrated experiment. It thus appears that at photon energies close to the onset of resonance there is a preferential emission of electrons along the occupied molecular-orbital axis. When the detector is along this direction the resonance-profile maximizes at photon energies just above onset; far away from this axis the profile displays only a shoulder at these energies.

This argument is only strictly correct for surface atoms. Electrons photoemitted along the c axis from a_{1g} orbitals in the bulk suffer refraction at the surface of the crystal and so emerge in a direction different from the c axis; electrons emitted from the a_{1g} orbitals of surface cations are not refracted. The refraction is a function of both the kinetic energy of the photoemitted electron (and, consequently, the photon energy) and the inner potential of the crystal. For 50-eV electrons and an inner potential of 20 eV, the deviation is estimated to be less than 20°. (See Ref. 6 for a discussion of the inner potential in these materials.) However, since there is a distribution of electron-emission directions around the c-axis direction, and since the photoemission spectra are particularly surface sensitive for photon energies around 50 eV, the changes observed in the $3d$ resonance profiles with angle of detection can be ascribed primarily to molecular-orbital effects.

The interpretation of the data presented thus far presupposes the existence of well-defined molecular orbitals for the d state in these materials. As discussed above, analysis of the intensity of the $3d$-emission features in the photoemission spectra leads to agreement with a molecular-orbital model. However, analysis of the variation in binding energy of these same features as a function of photon energy indicates the existence of delocalized d bands.[6] Indeed, since V_2O_3 is metallic and Ti_2O_3 is a narrow gap semiconductor, it is clear that a highly localized molecular-orbital picture of the electronic structure in these oxides cannot be appropriate for describing their transport properties. The coexistence in the photoemission spectra of evidence for both delocalized d bands and localized molecular orbitals indicates the complexity of the electronic structure of these oxides.

2. Localization

The cation $3d$ resonance profiles of Figs. 3 and 4 exhibit a delay in the onset of the $3p \rightarrow 3d$ resonance to photon

energies larger than the ground-state $3p \rightarrow 3d$ energy-level separation in both Ti_2O_3 and V_2O_3. The Ti $3p$ binding energy in Ti_2O_3 is 36.5 eV and the V $3p$ binding energy in V_2O_3 is 40.5 eV, as determined by photoemission.[27] Since both materials have empty d states at or close to E_F, the $3p \rightarrow 3d$ resonance would be expected to occur for photon energies close to these binding energies. It is clear from Figs. 3 and 4 that this is not the case. As discussed in Sec. III B, the $3p \rightarrow 3d$ resonance in Ti and V metals is also delayed;[2-4] the binding energy of the $3p$ level in Ti is 33 eV and in V, 37 eV. However, it is clear that the photon energy at which the profiles maximize in the angle-integrated measurement remains essentially unaffected by the change in $3p$ binding energy that occurs in going from the metal to the oxides; the $3d$ resonance profiles from both Ti and Ti_2O_3 maximize at 47 eV, those from V and V_2O_3 at close to 50 eV. This surprising result can be interpreted as evidence for the localized nature of the $[3p^5 3d^{n+1}]^*$ excited state in these materials.[3,4]

For $3p \rightarrow 3d$ optical absorption, the system goes from a $[3p^6 3d^n]$ ground state to a $[3p^5 3d^{n+1}]^*$ excited state. In going from a metal to a metal oxide the binding energy of the $3p$ state increases and, consequently, the $[3p^6 3d^n]$ ground-state energy changes. For the peak in the resonance profiles to occur at the same photon energy in both metal and oxide requires the excited-state energy to have changed by an equal amount. Since the ground-state energy change is due to decreased screening of the $3p$ core hole in the oxide, this result implies that the $[3p^5 3d^{n+1}]^*$ excited state experiences the same screening effect as does the ground state. This, in turn, implies that the excited state is highly localized on the same atom as the $3p$ hole in order that it experience the same change in screening.

This argument was originally presented by Bertel *et al.*,[3,4] who observed that the intensity of the O $2p$ emission from oxidized Ti ("TiO_2") went through a resonance as the photon energy was swept through the Ti $3p \rightarrow 3d$ transition, and that this resonance maximized at the same photon energy (47 eV) as that from the Ti $3d$ states. The resonance behavior of the O $2p$ emission is ascribed to hybridization of the O $2p$ states with Ti $3d$ states. Since in oxidized Ti there are no d electrons, Bertel *et al.*[3,4] infer indirectly the degree of localization of the $[3p^5 3d^{n+1}]^*$ state, using the arguments detailed above, from the resonance behavior of the O $2p$ emission. As will be discussed in Sec. VI B, the resonance emission from the O $2p$ states is not always similar to that from the cation $3d$ states in these $3d$-transition-metal oxides. (In V_2O_3, the O $2p$ emission peaks at approximately 8 eV lower photon energy than the V $3d$ emission.) Hence it is significant that by using nonmaximal valency oxides that have partially filled d states, we can *directly* measure the cation $3d$ resonance in the oxide, thus enabling the localization of the resonance to be separated from any hybridization effects.

The absolute binding energy of the $[3p^5 3d^{n+1}]^*$ excited state cannot be unambiguously determined from the $3d$ resonance profiles of either the metals or their oxides. Even where the resonance profile is well described by a Fano line shape, the binding energy of the excited state does not necessarily correspond to the maximum.[11] Where a Fano line shape is not observed, there is no quantitative way of determining this deviation. Hence arguments concerning the localization of the resonance that are based on the location (photon energy) of the maximum in a resonance profile must be treated with some caution. However, in the absence of a quantitative estimate of the difference between the peak in the profile and the transition energy, it is clear that no gross qualitative changes occur in the binding energy of the $[3p^5 3d^{n+1}]^*$ excited state relative to the $[3p^6 3d^n]$ ground state upon oxidation.

The maximum at 47 eV observed in the Ti $3d$ profile from Ti_2O_3 is consistent with the corresponding measurements from TiN_2,[17] $SrTiO_3$,[25] and TiS_2,[24] all of which show a similar resonance profile. Likewise, the V $3d$ profile for VN (Ref. 26) maximizes at 50 eV photon energy, similar to the profile from V_2O_3 measured here.

3. *Multielectron losses*

The large widths of the resonance profiles in the light transition metals have been explained by Barth *et al.*[2] as arising from multielectron losses excited during the $3p \rightarrow 3d$ optical absorption (see Sec. III). The width of the angle-integrated profile for the Ti $3d$ emission from Ti_2O_3 (Fig. 3) is similar to that measured for emission from Ti,[2-4] although there are some differences in the high-photon-energy structure of the profiles. The profiles of Refs. 2-4 were measured in a constant-initial-state (CIS) spectroscopy mode. In CIS the photon energy and detector-energy window are swept synchronously in order to count the electrons being emitted from only one initial state. Spurious features can appear in CIS profiles due to density-of-state effects or, in an angle-resolved mode, the dispersion of states into or out of the detection window. The resonance profiles presented here were determined from the integrated area above background of any particular emission feature in an EDC as the photon energy was varied. Another difference between the profiles measured in Ref. 2 and here is that no attempt was made here to correct for the transmission function of the spectrometers. This implies that the intensity at higher photon energies ($\simeq 60$ eV) in the profiles measured here is smaller than otherwise would be the case;[2] this is just the difference that is observed between Ti and Ti_2O_3. Finally, the relative decrease in emission at higher photon energies could be related to different shakeup mechanisms in the oxide as opposed to the metal.

Unlike Ti_2O_3, there are significant differences between the angle-integrated $3d$ resonance profiles from V_2O_3 and V. In fact, the profile from polycrystalline V (Ref. 2) taken in an angle-integrated mode resembles the normal-emission profile of V_2O_3 (Fig. 4) more than the angle-integrated profile, with both displaying a shoulder at the $3p \rightarrow 3d$ transition and maximizing at higher photon energies. We do not have an explanation for this curious result. The angle-integrated $3d$ profile from V_2O_3 shows only a single peak at the transition energy.

B. Oxygen $2p$ resonance

Under the assumption that the direct-recombination mechanism is purely intra-atomic, resonant photoemis-

sion can be used as a tool to isolate the d-state contribution to complex hybridized bands;[1] if only cation d states resonate upon sweeping the photon energy through the cation $3p \rightarrow 3d$ transition, then any observed resonance in the ligand emission must be due to d states hybridized with the ligand states. However, the data in Figs. 5 and 6 indicate that this application of resonant photoemission is not universally valid. The data obtained here on the resonance behavior of the O $2p$ emission from Ti_2O_3 and V_2O_3 cannot be explained in terms of the known hybridization properties of these oxides.

When the photon energy is swept through the Ti $3p \rightarrow 3d$ optical-absorption edge, the intensity of the O $2p$ emission from Ti_2O_3 doubles; the corresponding increases for the O $2p$ emission from V_2O_3 is less than half of that amount (Figs. 5 and 6). The conventional interpretation of resonant photoemission thus implies that there is considerably more d-state character in the O $2p$ band of Ti_2O_3 than in that of V_2O_3. However, this contradicts the accepted model of hybridization in these oxides.

The separation between the cation $3d$ and oxygen $2p$ bands is much smaller in V_2O_3 than in Ti_2O_3 (Figs. 1 and 2), which suggests greater cation-ligand wave-function mixing in V_2O_3. X-ray-diffraction studies[29] indicate that the hybridization should be roughly equivalent in these oxides. Finally, there is a larger chemical shift in the cation $2p$ binding energies in going from Ti to Ti_2O_3 than for V to V_2O_3;[9,10] this suggests a more ionic, less covalent bond in Ti_2O_3. Thus the overwhelming evidence is that the cation d states hybridize more with the O $2p$ states in V_2O_3 than in Ti_2O_3.

Resonant photoemission thus appears to fail to measure correctly the hybridization in these materials. What, then, is the origin of the dramatic resonance in the O $2p$ band in Ti_2O_3? A possible explanation would be interatomic direct recombination. Here the O $2p$ states themselves would resonate, not just the $3d$ states hybridized with the O $2p$ orbitals. This mechanism would consequently be nonlocal, similar to an interatomic Auger decay. The latter process has been shown to be important in photon- and electron-stimulated ion desorption from transition-metal-oxide surfaces.[30] Bertel *et al.*[11] discuss a similar mechanism, which they call cross autoionization, in the context of cation hybridization. If interatomic direct recombination is significant, we expect it to be more so in Ti_2O_3 than in V_2O_3 due to the increase in the number of d electrons available for conventional direct recombination in V_2O_3.[31] Surprisingly, the resonance behavior of the O $2p$ emission from oxidized Ti single crystals[3,4] does not show the dramatic resonance seen here in Ti_2O_3. This may be due to the relatively small amount of "TiO_2" formed in the oxidation. The resonance from the O $2p$ states in single-crystal TiO_2 is reported to be very strong.[32]

Unlike the cation $3d$ profiles measured from Ti_2O_3 and V_2O_3, the O $2p$ profiles show no significant angular effects. In Ti_2O_3 both the angle-integrated and normal-emission profiles (Fig. 5) peak at approximately 47 eV. This is the same energy as the $3p \rightarrow 3d$ resonance, as would be expected. In contrast, while the O $2p$ profiles from V_2O_3 measured in both angle-integrated and normal-emission modes peak at approximately 42 eV, this energy is almost 10 eV lower than the measured V $3p \rightarrow 3d$ transition. The origin of this dramatic shift in O $2p$ resonance maximum in V_2O_3 is as yet unknown.

VII. CONCLUSIONS

Resonant photoemission from cation $3d$ and O $2p$ states in both Ti_2O_3 and V_2O_3 has been observed as the photon energy is swept through the cation $3p \rightarrow 3d$ transition. These nonmaximal valency oxides are excellent materials in which to study the effect of a ligand environment on resonant photoemission from cation d states, due to the existence of partially occupied d states, well separated from the O $2p$ states. This investigation has revealed new aspects of the complexity of both the electronic structure of these oxides and the phenomenon of resonant photoemission in them. The major conclusions of this work are the following.

(i) Resonant photoemission from the cation $3d$ state in Ti_2O_3 and V_2O_3 displays a strong sensitivity to the molecular-orbital structure of these oxides. Results obtained using angle-resolved detection exhibit angular anisotropies in resonant photoemission which can be directly related of the molecular-orbital structure of the solid; such results have not previously been reported.

(ii) The maximum in the cation $3d$ resonance emission occurs at the same photon energy in both the metals[2-4] and these single-crystal oxides. This is interpreted, following Bertel *et al.*,[3-4] as evidence for a significant degree of localization of the cation resonance.

(iii) A strong resonance in the O $2p$ emission from Ti_2O_3 is observed as the photon energy is swept through the Ti $3p \rightarrow 3d$ transition. A much smaller resonance is seen in the O $2p$ emission from V_2O_3 at the V $3p \rightarrow 3d$ transition, despite an increased d character in the O $2p$ band in V_2O_3. This implies that caution must be used in extracting information on hybridization from resonant-photoemission data. A possible origin of the giant resonance in the O $2p$ states in Ti_2O_3 would be an interatomic direct recombination whereby the O $2p$ states themselves resonate.

ACKNOWLEDGMENTS

The authors are pleased to acknowledge R. J. Lad for his help during the course of the experiments and for many useful discussions. We would also like to thank R. F. Garrett, C. Hirschmugl, and G. P. Williams of the NSLS for invaluable technical assistance. The authors are indebted to V. E. Fowler for assistance with the manuscript. This work was partially supported by National Science Foundation–Solid State Chemistry Grant Nos. DMR-82-02727 and No. DMR-87-11423. Research was carried out at the National Synchrotron Light Source, Brookhaven National Laboratory, which is supported by the U.S. Department of Energy, Division of Materials Sciences and Division of Chemical Sciences (Grant No. DE-AC02-76-CH00016).

*Present address: Department of Physics, University of Oregon, c/o National Synchrotron Light Source, Brookhaven National Laboratory, Building 725-U4, Upton, NY 11973.

[1]L. C. Davis, J. Appl. Phys. **59**, R25 (1986), and references therein.

[2]J. Barth, F. Gerken, and C. Kunz, Phys. Rev. B **31**, 2022 (1985).

[3]E. Bertel, R. Stochbauer, and T. E. Madey, Phys. Rev. B **27**, 1939 (1983).

[4]E. Bertel, R. Stockbauer, and T. E. Madey, Surf. Sci. **141**, 355 (1984).

[5]A preliminary report of some of this work has been reported elsewhere: K. E. Smith and V. E. Henrich, Soild State Commun. (to be published).

[6]K. E. Smith and V. E. Henrich, Phys. Rev. B **38**, 5965 (1988).

[7]H. Kuwamoto, J. M. Honig, and J. Appel, Phys. Rev. B **22**, 2626 (1980).

[8]J. B. Goodenough, Prog. Solid State Chem. **5**, 145 (1972), and references therein.

[9]R. L. Kurtz and V. E. Henrich, Phys. Rev. B **25**, 3563 (1982).

[10]R. L. Kurtz and V. E. Henrich, Phys. Rev. B **28**, 6699 (1983).

[11]U. Fano, Phys. Rev. **124**, 1866 (1961); U. Fano and J. W. Cooper, Rev. Mod. Phys. **40**, 441 (1968).

[12]R. Bruhn, E. Schmidt, H. Schroder, and B. Sonntag, J. Phys. B **15**, 2807 (1980).

[13]J. Barth, F. Gerken, K. L. I. Kobayashi, J. H. Weaver, and B. Sonntag, J. Phys. C **13**, 1369 (1980).

[14]J. Barth, G. Kalkoffen, and C. Kunz, Phys. Lett. **74A**, 360 (1970).

[15]T. M. Zimkina, V. A. Fomichev, S. A. Gribovski, and I. I. Zhukova, Fiz. Tverd. Tela (Leningrad) **9**, 1447 (1967); **9**, 1490 (1967)] [Sov. Phys.—Solid State **9**, 1128 (1967); **9**, 1163 (1967)]; R. Haensel, P. Rabe, and B. Sonntag, Solid State Commun. **8**, 1845 (1970).

[16]J. L. Dehmer, A. F. Starace, U. Fano, J. Sugar, and J. W. Cooper, Phys. Rev. Lett. **26**, 1521 (1971); A. F. Starace, Phys. Rev. B **5**, 1773 (1972); J. Sugar, *ibid.* **5**, 1785 (1972); J. L. Dehmer and A. F. Starace, *ibid.* **5**, 1792 (1972).

[17]R. D. Bringans and H. Hochst, Phys. Rev. B **30**, 5416 (1984); P. A. P. Lindberg, L. I. Johansson, J. B. Lindström, and D. S. L. Law, Phys. Rev. B **36**, 939 (1987).

[18]J. M. McKay, M. H. Mohamed, and V. E. Henrich, Phys. Rev. B **35**, 4304 (1987).

[19]B. M. Biwer and S. L. Bernasek, Surf. Sci. **167**, 207 (1986).

[20]G. Zajec, S. D. Bader, A. J. Arko, and J. Zak, Phys. Rev. B **29**, 5491 (1984).

[21]F. J. Szalkowski, P. A. Bertrand, and G. A. Somorjai, Phys. Rev. B **9**, 3369 (1974).

[22]C. Wehenkel and B. Gauthe, Phys. Status Solidi B **64**, 515 (1974).

[23]B. Sonntag, R. Haensel, and C. Kunz. Solid State Commun. **7**, 597 (1969).

[24]Y. Ueda, H. Negishi, M. Koyano, M. Inoue, K. Soda, H. Sakamoto, and S. Suga, Solid State Commun. **57**, 839 (1986).

[25]N. B. Brooks, D. S. L. Law, T. S. Padmore, D. R. Warburton, and G. Thornton, Solid State Commun. **57**, 473 (1986).

[26]J. Lindstrom, P. A. P. Lindberg, L. I. Johansson, D. S. L. Law, and A. N. Christensen, Phys. Rev. B **36**, 9514 (1987).

[27]K. E. Smith, Ph.D. thesis, Yale University, 1988.

[28]C. Kunz, in *Photoemission in Solids II,* Vol. 27 of *Topics in Applied Physics,* edited by L. Ley and M. Cardona (Springer-Verlag, Berlin, 1979), p. 299.

[29]M. G. Vincent, K. Yvon, A. Gruttner, and J. Ashkenazi, Acta Crystallogr. Sect. A **36**, 803 (1980); M. G. Vincent, K. Yvon, and J. Ashkenazi, *ibid.* **36**, 808 (1980).

[30]For a review, see T. E. Madey, D. E. Ramaker, and R. Stockbauer, Annu. Rev. Phys. Chem. **35**, 215 (1984).

[31]J. A. D. Mathew and K. Komninos, Surf. Sci. **53**, 716 (1975).

[32]R. L. Kurtz (private communcation).